IFP Energies nouvelles International Conference
Rencontres Scientifiques d'IFP Energies nouvelles

This paper is a part of the hereunder thematic dossier published in OGST Journal, Vol. 67, No. 5, pp. 731-875 and available online here

Cet article fait partie du dossier thématique ci-dessous publié dans la revue OGST, Vol. 67, n° 5, pp. 731-875 et téléchargeable ici

Dossier edited by/Sous la direction de : **E. Rosenberg**
IFP Energies nouvelles International Conference/Rencontres Scientifiques d'IFP Energies nouvelles

Pore2Field - Flows and Mechanics in Natural Porous Media from Pore to Field Scale

Pore2Field - Physique des écoulements en milieux poreux naturels : de l'échelle du pore à l'échelle du réservoir

Oil & Gas Science and Technology – Rev. IFP Energies nouvelles, Vol. 67 (2012), No. 5, pp. 731-875

Oil & Gas Science and Technology – Rev. IFP Energies nouvelles, Vol. 67 (2012), No. 5, pp. 841-855

DOI: 10.2516/ogst/2012044

IFP Energies nouvelles International Conference
Rencontres Scientifiques d'IFP Energies nouvelles

Pore2Field - Flows and Mechanics in Natural Porous Media from Pore to Field Scale
Pore2Field - Physique des écoulements en milieux poreux naturels : de l'échelle du pore à l'échelle du réservoir

Evaluation of EnKF and Variants on the PUNQ-S3 Case

R. Valestrand[1*], G. Nævdal[1,2] and A.S. Stordal[1]

1 IRIS - International Research Institute of Stavanger, Thormølensgt. 55, 5008 Bergen - Norway
2 Department of Mathematics, University of Bergen, Postboks 7800, NO-5020 Bergen - Norway
e-mail: randi.valestrand@iris.no - Geir.Nævdal@iris.no - Andreas.S.Stordal@iris.no

* Corresponding author

Résumé — Évaluation de l'EnKF et des variantes du cas PUNQ-S3 — Au cours de la dernière décennie, le filtre de Kalman d'Ensemble (EnKF, *Ensemble Kalman Filter*) a attiré l'attention en tant que méthode prometteuse pour résoudre le problème de calage d'historique de réservoir, à savoir l'actualisation des paramètres de modèle de sorte que la sortie de modèle corresponde aux données de production mesurées. La méthode présente des qualités uniques dans la mesure où elle procure des actualisations en temps réel et une quantification d'incertitude de l'estimation, peut estimer toute propriété physique disponible, et est facile à mettre en œuvre. Elle présente toutefois ses limitations : en particulier, elle est fondée sur une hypothèse d'une distribution gaussienne de variables et d'erreurs de mesure. Plusieurs affinements ont été proposés pour surmonter les points faibles de l'EnKF. Ces affinements sont, toutefois, principalement testés sur des cas synthétiques concernant un point faible à la fois, ne contenant ou ne combinant pas la complexité et la non-linéarité élevée d'un cas de champ réel. Dans cet article, nous étudions certaines des méthodes affinées sur un réservoir non linéaire, le modèle 3D, triphasé, PUNQ-S3. Nous comparons la performance de l'EnKF original avec la performance du filtre racine carrée d'ensemble (EnSRF, *ensemble square root filter*), une méthode EnKF avec localisation désignée sous le nom de filtre de Kalman d'ensemble hiérarchique (HEnKF, hierarchical *ensemble Kalman filter*), et le filtre mélange gaussien adaptatif (AGM, *adaptive Gaussian mixture*). Autant que nous sachions, il s'agit de la première fois que l'EnKF et l'EnSRF ont été comparés dans un cas de champ non linéaire de dimension élevée. Dans l'ensemble, nous constatons que l'AGM et le HEnKF fonctionnent mieux que l'EnSRF et l'EnKF. L'EnSRF semble présenter une performance légèrement meilleure que l'EnKF. Toutefois, l'introduction d'une procédure de localisation (telle que dans le HEnKF) semble avoir beaucoup plus d'influence que le remplacement de l'EnKF par l'EnSRF. En comparant les deux meilleures méthodes, l'AGM est préférable à l'HEnKF, à la fois quand il s'agit de préserver la géologie initiale de l'ensemble et pour la cohérence des prédictions.

Abstract* — *Evaluation of EnKF and Variants on the PUNQ-S3 Case — *Over the last decade the ensemble Kalman filter (EnKF) has attracted attention as a promising method for solving the reservoir history matching problem: updating model parameters so that the model output matches the measured production data. The method possesses unique qualities, such as; it provides real-time updates and uncertainty quantification of the estimate, it can estimate any physical property at hand and it is easy to implement. The method does, however, have its limitations; in particular, it is derived based on an assumption of a Gaussian distribution of variables and measurement errors. Several refinements have been proposed to overcome the shortcomings of the EnKF. These refinements are, however, mainly tested on synthetic cases addressing one shortcoming at a time, not containing or combining the*

complexity and the high nonlinearity of a real field case. In this paper, we investigate some of the refined methods on a nonlinear reservoir, the 3D, three-phase, PUNQ-S3 model. We compare the performance of the original EnKF with the performance of the ensemble square root filter (EnSRF), an EnKF method with localization, which is named the hierarchical ensemble Kalman filter (HEnKF) and the newly proposed Adaptive Gaussian Mixture filter (AGM). To the best of our knowledge, this is the first time the EnKF and the EnSRF have been compared on a high-dimensional nonlinear field case. Overall, we see that the AGM and HEnKF work better than the EnSRF and EnKF. The EnSRF seems to have a slightly better performance than the EnKF. However, the introduction of a localization procedure (as in the HEnKF) seems to be much more influential than replacing the EnKF with the EnSRF. Comparing the top two methods, the AGM is preferable over the HEnKF, both when it comes to preserving the initial geology of the ensemble and to the consistency of the predictions.

INTRODUCTION

Petroleum production is a challenging task in many ways. To be able to optimize petroleum production, when it comes to both the economic and environmental aspects, it is important to know as much as possible about the reservoir at hand. History matching of reservoir properties from well data has been an important tool in the petroleum industry for decades, improving production decision-making when it comes to, *e.g.*, quantifying remaining oil volumes, determining their location in the reservoir, and optimal placement of wells and well trajectories.

The Ensemble Kalman filter (EnKF) was first introduced in the atmospheric and oceanographic sciences by Evensen [1] as a solution for the Kalman filter equations for large-scale nonlinear systems. The EnKF is a data assimilation method where the essence is to update an ensemble of models by means of measured data. The method is suitable for real-time applications, provides an uncertainty estimate and is easy to implement. Its first use in petroleum science was in Lorentzen *et al.* [2], where a fluid-flow well model was tuned, and shortly after, in Nævdal *et al.* [3], it was used to tune the permeability field of a near-well reservoir model. Since then, many papers using the EnKF methodology in reservoir applications, including field studies, have been published; *e.g.*, Haugen *et al.* [4], Evensen *et al.* [5], and Bianco *et al.* [6]. For a review on the use of EnKF in reservoir engineering see Aanonsen *et al.* [7], and for more recent developments and applications see Seiler *et al.* [8], Chen and Oliver [9] and Lorentzen *et al.* [10].

Despite the success stories of using the EnKF for reservoir applications, the method has its limitations. In particular, it is derived based on an assumption of a Gaussian distribution of variables and measurement errors. The computational time issue forces us to use relatively small ensembles, which results in spurious correlations (updates typically outside the sensitivity area not caused by information in the data). Also, it has been shown that the method may encounter severe problems when used on highly nonlinear models, see *e.g.*, Verlaan and Heemink [11].

In this paper, we compare the EnKF with the Ensemble Square Root Filter (EnSRF), an EnKF method with localization, the Hierarchical Ensemble Kalman Filter (HEnKF), and the newly proposed Adaptive Gaussian Mixture filter (AGM). The ensemble square root filter was introduced by Bishop *et al.* [12] and Tippett *et al.* [13] to avoid the sampling error due to the stochastic perturbations added to the observations in the traditional EnKF. In this paper, we present, for the first time, a comparison of the EnKF and the EnSRF in a high-dimensional nonlinear field case. Localization methods are used to avoid/dampen the spurious correlations and in this paper, we investigate an adaptive localization method, the HEnKF, described in Vallès and Nævdal [14], which was proposed by Anderson [15]. The method is based on calculating the Kalman gain for several subensembles of the total ensemble and dampen updates that are not consistent among the Kalman gains. The method is adaptive in the sense that the dampening factor is computed based solely on the ensemble itself. Finally, in this comparison of methods we include the AGM, introduced in Stordal *et al.* [16], which combines the advantages of a particle filter with the EnKF. As in particle filters each ensemble member has an assigned weight which is updated at each assimilation step: in addition, a dampening factor is included in the Kalman gain update to perform smaller linear steps than the EnKF. The dampening factor is case-dependent, *i.e.*, it depends on how linear/nonlinear the model is.

To analyze the performance of the different filters, taking into account the Monte Carlo effect, each method is tested on the reservoir using several initial ensembles. The results are evaluated by statistical measures considering the history match, the estimated ensemble and the predictability when forecasting.

This paper is organized as follows: in Section 1 an introduction to the different filters is given, then, in Section 2 the statistical measures for validating the results are given and

discussed. In Section 3 the reservoir case is introduced and the results are presented and discussed.

1 DESCRIPTION OF THE FILTER METHODS INVESTIGATED

In this section, we will give a short description of the four different filter methods and refer to papers giving a more extensive description of the methods.

1.1 The Ensemble Kalman Filter

The equations for the EnKF we have tested here are based on the EnKF methodology originally tested on reservoir applications in Nævdal *et al.* [3]; a short description follows. The EnKF repeatedly switches between the forecast step and the analysis step. The forecast step consists of running the forward model, f, (*i.e.*, the simulator solving the reservoir flow equations) from the current assimilation time to the next for each ensemble member. For the ith member of the ensemble at time level k, we denote the forecasted state vector by $\mathbf{X}^f_{k,i}$ and the analyzed state by $\mathbf{X}^a_{k,i}$ (in the following, we use the superscripts a and f for analyzed and forecasted, respectively). The state vector can be written as:

$$\mathbf{X}_{k,i} = \begin{bmatrix} \mathbf{s}_{k,i} \\ \mathbf{p}_{k,i} \\ \mathbf{d}_{k,i} \end{bmatrix} \tag{1}$$

where $\mathbf{s}_{k,i}$ is a column vector of what we treat as static model parameters (*e.g.* porosity and permeability fields), $\mathbf{p}_{k,i}$ is a column vector of dynamic model parameters (*e.g.*, pressure and saturation fields) and $\mathbf{d}_{k,i}$ denotes the simulated well measurements. The forecast step is given by:

$$\mathbf{X}^f_{k,i} = f(\mathbf{X}^a_{k-1,i}) \tag{2}$$

During the forecast step the model parameters will be kept constant while the dynamic variables and well measurements are developing as a function of the fluid flow. The method is based on a linear relationship between the simulated measurements, $\mathbf{d}_k$, and the states, $\mathbf{X}_k$:

$$\mathbf{d}_{k,i} = \mathbf{H}\mathbf{X}_{k,i} \tag{3}$$

where $\mathbf{H}$ is a mapping matrix consisting of ones and zeros.

In the analysis step, the model parameters and the dynamic variables of the state vector are updated. At each assimilation time k, the forecast mean, $\underline{\mathbf{x}}^f_k$, and an approximation of the forecast error covariance matrix, $\mathbf{P}^f_k$, can be calculated from the forecasted state, $\mathbf{X}^f_k$, which holds N_e members with member i as column i. The mean and covariance matrix are calculated using:

$$\underline{\mathbf{x}}^f_k = \frac{1}{N_e}\sum_{i=1}^{N_e}\mathbf{X}^f_{k,i} \tag{4}$$

$$\mathbf{P}^f_k = \frac{1}{(N_e-1)}\mathbf{A}^f_k(\mathbf{A}^f_k)^T \tag{5}$$

where $\mathbf{A}_k$ is the ensemble anomalies defined as $\mathbf{A}_{k,i} = \mathbf{X}_{k,i} - \underline{\mathbf{x}}_k$. Using the results of Equations (4, 5), the analyzed ensemble members can be calculated by the update equation:

$$\mathbf{X}^a_{k,i} = \mathbf{X}^f_{k,i} + \mathbf{K}_k(\mathbf{d}^{obs}_k + \mathbf{D}_{k,i} - \mathbf{H}\mathbf{X}^f_{k,i}) \tag{6}$$

where the Kalman gain matrix, $\mathbf{K}_k$, is given by:

$$\mathbf{K}_k = \mathbf{P}^f_k\mathbf{H}^T(\mathbf{H}\mathbf{P}^f_k\mathbf{H}^T + \mathbf{R}_k)^{-1} \tag{7}$$

and $\mathbf{d}^{obs}$ is the measurements. We assume that the measurement noise has a multinormal distribution with zero mean and covariance matrix $\mathbf{R}_k$ (the covariance matrix of the measurement noise might be time-dependent). Finally, the updated mean, $\underline{\mathbf{x}}^a_k$, and an approximation to the updated covariance matrix, $\mathbf{P}^a_k$, are calculated from the updated ensemble:

$$\underline{\mathbf{x}}^a_k = \frac{1}{N_e}\sum_{i=1}^{N_e}\mathbf{X}^a_{k,i} \tag{8}$$

$$\mathbf{P}^a_k = \frac{1}{(N_e-1)}\mathbf{A}^a_k(\mathbf{A}^a_k)^T \tag{9}$$

In Equation (6), random noise $\mathbf{D}_{k,i}$ is added to $\mathbf{d}_k$ to treat the measurements as random variables. It was shown independently in Burgers *et al.* [17] and Houtekamer and Mitchell [18] that adding the random noise, $\mathbf{D}_{k,i}$, is required to get the correct posterior covariance matrix for a linear model asymptotically. In other words, if $N_e \to \infty$ the updated error covariance matrix matches the theoretical value given by the Kalman filter:

$$\mathbf{P}^a_k = (\mathbf{I} - \mathbf{K}_k\mathbf{H})\mathbf{P}^f_k$$

The practice of adding random noise in Equation (6) has its drawbacks. Whitaker and Hamil [19] showed that adding the random noise, $\mathbf{D}_{k,i}$, introduces a sampling error, especially for small ensemble sizes. To solve this problem a group of filters identified as "ensemble square root filters" have been developed.

1.2 The Ensemble Square Root Filter

The Ensemble Square Root Filter (EnSRF) uses a different updating scheme than the EnKF which avoids introducing the random noise term, $\mathbf{D}_{k,i}$, into Equation (6). Bishop *et al.* [12] and Tippett *et al.* [13] were some of the first to propose a method where the updated error covariance matrix matches the theoretical one and hence one avoids the sampling problem. The EnSRF is also called a deterministic filter as random noise is not added to the measurements, contrary to the EnKF, which is called a stochastic filter. Two main steps differ in the EnSRF compared with the EnKF: the ensemble mean is updated with the standard

Kalman filter analysis equation and the ensemble anomalies are transformed so that the updated error covariance matrix matches the theoretical one. In our study, we have used the symmetric transformation solution described in Sakov and Oke [20]. Below is a description along the lines of Sakov and Oke [20].

The mean of the ensemble is updated by the analysis equation:

$$\underline{\mathbf{x}}_k^a = \underline{\mathbf{x}}_k^f + \mathbf{K}_k(\mathbf{d}_k^{obs} - \mathbf{H}\underline{\mathbf{x}}_k^f) \tag{10}$$

and the ensemble anomalies are transformed by the symmetric transformation matrix, $\mathbf{T}^s$:

$$\mathbf{A}_k^a = \mathbf{A}_k^f \mathbf{T}_k^s \tag{11}$$

so that the update error covariance matrix matches the theoretical one. The update covariance matrix can be written as:

$$\mathbf{P}_k^a = \frac{1}{(N_e-1)}\mathbf{A}_k^a(\mathbf{A}_k^a)^T = \frac{1}{(N_e-1)}\mathbf{A}_k^f\mathbf{T}_k^s(\mathbf{A}_k^f\mathbf{T}_k^s)^T \tag{12}$$

and the theoretical covariance matrix can be written as:

$$\mathbf{P}_k^a = (\mathbf{I}-\mathbf{K}_k\mathbf{H})\mathbf{P}_k^f = (\mathbf{I}-\mathbf{K}_k\mathbf{H})\frac{1}{(N_e-1)}\mathbf{A}_k^f(\mathbf{A}_k^f)^T \tag{13}$$

By setting the right-hand sides of Equations 12 and 13 equal, we get the equation that the transformation matrix should fulfill:

$$\mathbf{A}_k^f\mathbf{T}_k^s(\mathbf{A}_k^f\mathbf{T}_k^s)^T = (\mathbf{I}-\mathbf{K}_k\mathbf{H})\mathbf{A}_k^f(\mathbf{A}_k^f)^T \tag{14}$$

It can be shown that the general form of $\mathbf{T}$ that satisfies Equation (14) is:

$$\mathbf{T}_k = \mathbf{T}_k^s\mathbf{U} \tag{15}$$

where $\mathbf{U}$ is an arbitrary orthonormal matrix ($\mathbf{U}\mathbf{U}^T = \mathbf{I}$) and:

$$\mathbf{T}_k^s = [\mathbf{I} - \frac{1}{N-1}(\mathbf{H}\mathbf{A}_k^f)^T\mathbf{R}^{-1}\mathbf{H}\mathbf{A}_k^f]^{-1/2} \tag{16}$$

Performing an eigenvalue decomposition of the matrix in the square brackets:

$$\mathbf{I} - \frac{1}{N-1}(\mathbf{H}\mathbf{A}_k^f)^T\mathbf{R}^{-1}\mathbf{H}\mathbf{A}_k^f = \mathbf{C}\boldsymbol{\Gamma}\mathbf{C}^T \tag{17}$$

the solution for $\mathbf{T}_k^s$ is:

$$\mathbf{T}_k^s = \mathbf{C}\boldsymbol{\Gamma}^{-1/2}\mathbf{C}^T \tag{18}$$

Equation (18) is shown to preserve the mean, Sakov and Oke [20], and is referred to as the symmetric solution. Mean preservation is important to avoid underestimation of the system error covariance, which can lead to divergence of the filter, Julier and Uhlmann [21].

1.3 The Hierarchical Ensemble Kalman Filter

Whereas the square root filter is introduced to reduce the sampling effect from the noise $\mathbf{D}_{k,i}$ added to the measurements (*see Eq. 6*), the Hierarchical Ensemble Kalman Filter (HEnKF) was developed to reduce the spurious correlations that are introduced into $\mathbf{P}_k^f$ since we are working with a small ensemble size. Methods developed to reduce these effects are named localization methods, as the problem was first noticed by the tendency for the EnKF to update states located at a far distance from the observations. The HEnKF is one of several localization methods that have been suggested. The strength of the HEnKF is that it is an adaptive localization method.

The spurious correlations in the forward error covariance matrix are propagated into the Kalman gain matrix and a dampening is suggested to reduce this effect. The spurious correlations cause updates of the states in regions where it is not warranted by the data. The hierarchical ensemble Kalman filter used here is based on the hierarchical ensemble filter introduced by Anderson [15]. The implementation used in this work follows the one used in Vallès and Nævdal [14].

The idea of the HEnKF is to divide the ensemble into sub-ensembles, use the traditional EnKF algorithm on each sub-ensemble and identify spurious correlation by comparing the Kalman gain calculated from the different sub-ensembles. Those entries of the Kalman gain that come out very different for each sub-ensemble are believed to be dominating by random effects causing spurious correlations and will therefore be dampened.

As proposed by Anderson [15], a dampening factor between 0 and 1 is calculated from the sub-ensembles at each assimilation step. This factor is defined to minimize the expected root mean square difference between the calculated Kalman gain matrices for each sub-ensemble. This minimization results in a dampening factor, $\alpha_{(m,n)}$, that is calculated for each entry of the Kalman gain, and is chosen to be positive and defined by:

$$\alpha_{(m,n)} = \max\left[\left(\frac{\frac{\left(\sum_{i=1}^{N_g}\kappa_{k,i}\right)^2}{\sum_{i=1}^{N_g}\kappa_{k,i}^2} - 1}{(N_g-1)}\right), 0\right] \tag{19}$$

where $\kappa_{k,i}$ is the (m,n) entry of the Kalman gain matrix for the ith sub-ensemble at time k and N_g is the number of sub-ensembles. Finally, a matrix $\mathbf{B}_k$ of the same size as the Kalman gain is defined with $\alpha_{(m,n)}$ as its (m,n) entry. Each sub-ensemble is updated by:

$$\mathbf{X}_{k,i,j}^a = \mathbf{X}_{k,i,j}^f + \mathbf{B}_k \circ \mathbf{K}_k(\mathbf{d}_k^{obs} + \mathbf{D}_{k,i,j} - \mathbf{H}\mathbf{X}_{k,i,j}^f)$$
$$\forall i \in \left[1,\ldots,N_{e_{sub}}\right], \forall j \in \left[1,\ldots,N_g\right] \tag{20}$$

where $N_{e_{sub}}$ is the number of ensemble members in each sub-ensemble. The ∘ denotes the entry wise (Schur) product between two matrices. The updated ensemble at each time step consist of all the updated sub-ensembles:

$$\mathbf{X}^a = \begin{bmatrix} \mathbf{X}^a_{j=1} & \mathbf{X}^a_{j=2} & \dots & \mathbf{X}^a_{N_g} \end{bmatrix} \tag{21}$$

The updated mean and the updated covariance can be calculated from the updated ensemble as in the original EnKF methodology; see Equations (8, 9).

1.4 Adaptive Gaussian Mixture Filter

The Adaptive Gaussian Mixture filter (AGM) used in this work was first presented in Stordal *et al.* [16]. The AGM loosens up the requirement of a linear/Gaussian model by making a smaller linear update than the EnKF and takes advantage of the information contained in the importance weights, w, which are standard in particle filters, while keeping the computational costs as low as the EnKF. The AGM is hence a more robust filter when it comes to handling non-Gaussian priors and nonlinear models, which are both often the case in reservoir modeling. To loosen up the requirement of a Gaussian prior, importance weights, w, are assigned to each of the ensemble members.

Following are the main steps of the AGM. The forecast ensemble mean is calculated as:

$$\underline{\mathbf{x}}^f_k = \frac{1}{N_e} \sum_{i=1}^{N_e} \mathbf{X}_{i,k} \tag{22}$$

and the forecast error covariance matrix is given by:

$$\mathbf{P}^f_k = \frac{h^2}{(N_e - 1)} \mathbf{A}^f_k (\mathbf{A}^f_k)^T \tag{23}$$

The bandwidth parameter, h, causes the filter to perform smaller linear updates than the EnKF. The selection of h is case-dependent as different cases possess different degrees of nonlinearity (*e.g.*, number of phases, dimensions and number of wells). The value must be chosen by the user. If set to one Equation (23) equals Equation (5) and the only difference between the AGM and the EnKF is that in the AGM the weights are calculated. $h = 1$ works well for close to linear models (as so does the EnKF). If $h = 0$, the AGM reduces to a particle filter. We know that applying pure particle filters to reservoir problems are not feasible due to, *e.g.*, the computational cost associated with being forced to use much more than a hundred ensemble members and the problem of filter degeneracy in high-dimensional systems; see Stordal *et al.* [16] for more details. Using the AGM on a reservoir model requires taking advantage of both the Kalman update step and the weighting step, hence $h \in < 0, 1 >$. Based on our knowledge so far we advise using $h \in [0.2, 0.6]$ for reservoir models and chose values closer to 0.2 for strongly nonlinear models and values closer to 0.6 for less nonlinear models.

The analyzed ensemble is given by:

$$\mathbf{X}^a_{k,i} = \mathbf{X}^f_{k,i} + \mathbf{K}_k(\mathbf{d}^{obs}_k + \mathbf{D}_{k,i} - \mathbf{H}\mathbf{X}^f_{k,i}) \tag{24}$$

where the Kalman gain matrix, $\mathbf{K}_k$, is given by:

$$\mathbf{K}_k = \mathbf{P}^f_k \mathbf{H}^T (\mathbf{H}\mathbf{P}^f_k \mathbf{H}^T + \mathbf{R}_k)^{-1} \tag{25}$$

Finally, the analyzed mean, $\underline{\mathbf{x}}^a_k$, and analyzed covariance matrix, $\mathbf{P}^a_k$, are calculated from the analyzed ensemble:

$$\underline{\mathbf{x}}^a_k = \frac{1}{N_e} \sum_{i=1}^{N_e} \mathbf{X}^a_{k,i} \tag{26}$$

$$\mathbf{P}^a_k = \frac{h^2}{(N_e - 1)} \mathbf{A}^a_k (\mathbf{A}^a_k)^T \tag{27}$$

Note the importance weights do not enter into any of the equations above in the implementation used in this work. The weights are, however, updated at each assimilation step as described below and used when validating the estimated result obtained by the AGM (see, *e.g.*, *Eq. 32*). In the notation below, $\mathbf{w}$ is the vector holding the N_e weights:

$$\mathbf{w}_{k,i} = \mathbf{w}_{k-1,i} \Phi(\mathbf{d}^{obs}_k + \mathbf{D}_{k,i} - \mathbf{H}\mathbf{X}^f_{k,i}, \mathbf{H}\mathbf{P}^f_k \mathbf{H} + \mathbf{R}_k) \tag{28}$$

where Φ denotes the multivariate normal probability density function. Then the weights are normalized:

$$\mathbf{w}_{k,i} = \frac{\mathbf{w}_{k,i}}{\sum_{j=1}^{N_e} \mathbf{w}_{k,j}} \tag{29}$$

and the range is reduced (to avoid weight collapse for small values of h):

$$\mathbf{w}_{k,i} = \alpha \mathbf{w}_{k,i} + (1 - \alpha) N_e^{-1} \tag{30}$$

where $\alpha = N_e^{-1} N_{eff}$ and N_{eff} is the effective ensemble size given by $N_{eff} = \frac{1}{\sum_{i=1}^{N_e} \mathbf{w}^2_{k,i}}$.

In this work, we do not use resampling of the ensemble. Note that in addition to the updating of the weights, the equations above do differ from the basic EnKF equations in Section 1.1 by the term h^2 in Equations (23, 27).

2 VALIDATION METHODS

The attempt in this study is to compare the performance of the four methods on a reservoir case. To be able to decide which method performs best, we must discuss what we consider to be a good filter estimate and use criteria to validate the results thereafter. A traditional way of considering the goodness of an estimated model is to run it through the history and calculate the root mean square difference

between the model response and the measurements; a measure of the history match of the measurements. This measure is also known as the objective function. This evaluation technique is standard in traditional history matching where the final estimate consists of one model and the rule of validation is: the smaller the root mean square difference measure obtained the better the estimate. A criterion for a "good" match is also clear in this one-model history matching; the root mean square difference measure should be explained by the measurement error alone.

When dealing with filter methods, we also typically rerun the estimated ensemble through the history and compute the root mean square differences between the ensemble of responses and the measurements. In this work, we calculate the objective function, J, after such a rerun by:

$$J = \sqrt{\frac{1}{N_d N_e}\sum_{i=1}^{N_e}\sum_{j=1}^{N_d}\left(\frac{\mathbf{d}_j^{obs} - \mathbf{c}_{i,j}}{\sigma_j}\right)^2} \tag{31}$$

where N_e is the number of ensemble members, N_d is the number of measurements (*i.e.*, all data types at all times) and $\mathbf{c}_{i,j}$ is the reservoir model's response to the measured data, using the estimated ensemble as input. When calculating the history match for the AGM results, the weights are included so that each ensemble member's contribution to J is weighted;

$$J = \sqrt{\frac{1}{N_d}\sum_{i=1}^{N_e}\sum_{j=1}^{N_d} w_i\left(\frac{\mathbf{d}_j^{obs} - \mathbf{c}_{i,j}}{\sigma_j}\right)^2} \tag{32}$$

where $\sum_{i=1}^{N_e} w_i = 1$.

Regarding the evaluation of the objective function value, it is not as simple as for the traditional history matching mentioned above. This is obvious from the following: if the lowest value was desired this could be achieved by an ensemble where each member provided the exact same history match and which also matched the measurements. The latter is what we refer to as ensemble collapse, which can be caused by, *e.g.*, insensitivity: clearly this is not desirable. So, what is the "good" value to obtain from Equation (31)? From a statistical point of view the optimal solution is achieved if the estimated ensemble corresponds to the true posterior distribution, given all the measurements. If we had a sample from the true posterior distribution, we could run it through the history and calculate the value Equation (31) should approach. The problem is that we do not know the true posterior distribution and that it is too expensive to calculate it for real reservoir cases.

So far we have discussed validating measures related to the history match produced by rerunning the estimated ensemble. It is also common to investigate the ensemble parameter values themselves. A very common measure, when dealing with synthetic studies, is the root mean square error between the estimated ensemble and the true (*e.g.*, permeability and porosity of every grid block). The root mean square error at each assimilation time and for each analyzed static variable in the state vector, $\mathbf{s}^a$, is given by:

$$\text{RMSE} = \sqrt{\frac{1}{N_e N_g}\sum_{i=1}^{N_e}\sum_{k=1}^{N_g}\left(\mathbf{s}_{k,i}^a - \mathbf{s}^{true}\right)^2} \tag{33}$$

In this work, we also calculate a measure for the distance from the truth; we calculate the distance between the mean ensemble and the truth for each static variable in the state vector at each assimilation time:

$$\text{DistMeanTrue} = \sqrt{\frac{1}{N_g}\sum_{k=1}^{N_g}\left(\mathbf{s}^{true} - \underline{\mathbf{s}}_k^a\right)^2} \tag{34}$$

For real reservoir cases the latter two validating measures are not applicable and we propose instead to use two other measures. As mentioned above, it is desirable to maintain the ensemble spread. A measure of the ensemble spread is the distance from the analyzed mean of the estimated ensemble, $\underline{\mathbf{s}}^a$, to the ensemble members:

$$\text{EnsSpread} = \sqrt{\frac{1}{N_e N_g}\sum_{i=1}^{N_e}\sum_{k=1}^{N_g}\left(\mathbf{s}_{k,i}^a - \underline{\mathbf{s}}^a\right)^2} \tag{35}$$

for each variable in the state vector at each assimilation time. The final measure is derived by the claim that selecting between two solutions with the same history match, the solution which is closer to the prior distribution is the better one. As the initial ensemble is a sample from the prior distribution, we therefore suggest measuring the distance between the initial ensemble, $\mathbf{s}^{ini}$, and the analyzed ensemble:

$$\text{DistIni} = \sqrt{\frac{1}{N_e N_g}\sum_{i=1}^{N_e}\sum_{k=1}^{N_g}\left(\mathbf{s}_{k,i}^a - \mathbf{s}_{k,i}^{ini}\right)^2} \tag{36}$$

The measure is calculated for each variable in the state vector at each assimilation time.

Next, we evaluate the performance of the four filters on the PUNQ-S3 case.

3 THE PUNQ-S3 TEST CASE

The case considered is a 3D, 3-phase reservoir: the PUNQ-S3 test case. The PUNQ-S3 test case was used in a comparative study and is fully described in Floris *et al.* [22], and the data set is available on PUNQ-S3 website of the Imperial College of London [23]. The model is based on a real field and contains $19 \times 28 \times 5$ gridblocks, of which 1 761 are active. The field is bounded to the east and south by a fault and links to the north and west to a fairly strong aquifer.

The field initially contains a gas cap and an oil rim. Due to the strong aquifer the oil is produced by primary depletion and the only wells are six production wells. The production schedule consists of two periods. First, there is an 8-year history match period consisting of 1 year of well testing, 3 years of field shut-in and 4 years of field production. The second period is an 8.5-year prediction period with shut-in tests every year.

In this example, we estimate the porosity and the horizontal and vertical permeability and update the dynamic fields: pressure, water and gas saturation and the solution gas-oil ratio. The true porosity and permeability were downloaded from the website along with information about the timing of the observations from the six wells and their uncertainties. The actual observations are regenerated using the current version of the reservoir simulator (Eclipse). The well measurements include bottom hole pressures, gas-oil ratios and water cuts.

We applied the sequential Gaussian simulation method (sgsim) for generating the porosity realizations and the sequential Gaussian cosimulation method (sgcosim) to produce the permeability realizations, both from the GSLIB (Deutsch and Journel [24]). The permeability and porosity are correlated with a correlation coefficient of 0.8. These methods are also used when generating the true fields presented in the original data set. The generated porosity and permeability fields now take into account the knowledge about the reservoir collected from logs, cores, seismic and general geological information since this information is used to generate geostatistical parameters such as principal directions, correlation lengths and anisotropy ratios. The porosity and permeability are also conditioned to the values obtained from core samples at the well locations. The PUNQ-S3 case encompasses 5 layers and these layers are independent.

TABLE 1

Initial ensembles generated for the PUNQ-S3 study

10 ensembles with 100 members
10 ensembles with 200 members
1 ensemble with 1 000 members
1 ensemble with 2 000 members

Table 1 gives an overview of the ensembles generated in this study. The ensembles with 100 and 200 members are generated independently, while the one with 1 000 members consist of the 10 ensembles with 100 members and the one with 2 000 members consist of the 10 ensembles with 200 members. Figure 1 shows the logarithm of the true horizontal permeability for the 5 layers in the left column. The mean of the initial ensemble for one of the ensembles with 100 members and its standard deviation are shown in the middle and right column, respectively. The right column shows that all layers have zero variance at the placement of the 6 wells, which follows from the fact that the generated fields are constrained to the well data (the wells are plotted as white dots in the layers where they are completed). We can notice that the initial ensemble is very good, *i.e.*, the main trends of the true field can be spotted and this is the case for all the 22 ensembles generated. Also, a good initial ensemble will make the estimation problem close to linear. Some may argue that this makes the PUNQ-S3 case an easy test case, as the mean of the initial ensemble already gives a pretty good history match (shown later). This is, however, how we ideally would like our initial ensembles to be even though it might be hard to achieve for real field cases. Also, the PUNQ-S3 case is one of the few field-like cases which is well known, available, 3D, 3-phase, based on a real field and which has a history match period and a prediction period that are well defined. This makes it a perfect choice for the study in this paper as long as we can distinguish the results of the different methods compared.

We use the first period to estimate the static fields by the four filter methods, all methods are used for all the 22 ensembles. The results of the history match period are validated by the statistical measures in Section 2. For the AGM the parameter h was, after some testing, chosen to be 0.4. The testing was done by performing the estimation on one of the 22 ensembles, using 3 different h values (0.2, 0.4 and 0.6), and the h value giving the best history match was used for the study. The PUNQ-S3 case is nonlinear due to 3 dimensions and 3 phases but the good initial ensemble makes the estimation problem more linear. In light of this an intermediate h value such as 0.4 seems reasonable for this study. For the HEnKF, we used 5 sub-ensembles.

The second period is used to forecast uncertainty in the cumulative oil production at 16.5 years, assuming production from the 6 wells only, each well having a target oil rate of 150 sm^3/d and a minimum bottom hole flowing pressure of 120 bar. First, we will show the results from the history match period and then we will compare the predicted cumulative oil production at 16.5 years.

Figure 2 shows the objective function values (*Eq. 31, 32*) for the 22 estimations performed with each filter. The values connected with solid lines correspond to the values obtained using the ensembles with 100 members, the values connected with dashed lines correspond to the ones with 200 members, the dots at $x = 11$ correspond to the ones with 1 000 members and finally, the dots at $x = 12$ correspond to the ones with 2 000 members. All the colored values correspond to a very good history match and are closely distributed around 1.5. The corresponding values for the initial ensembles are shown in black and are distributed around 14. Table 2 summarizes the results in Figure 2, it shows the mean and standard deviation over 10 ensembles for each method (except for the ensembles with 1 000 and 2 000 members where we only have one ensemble).

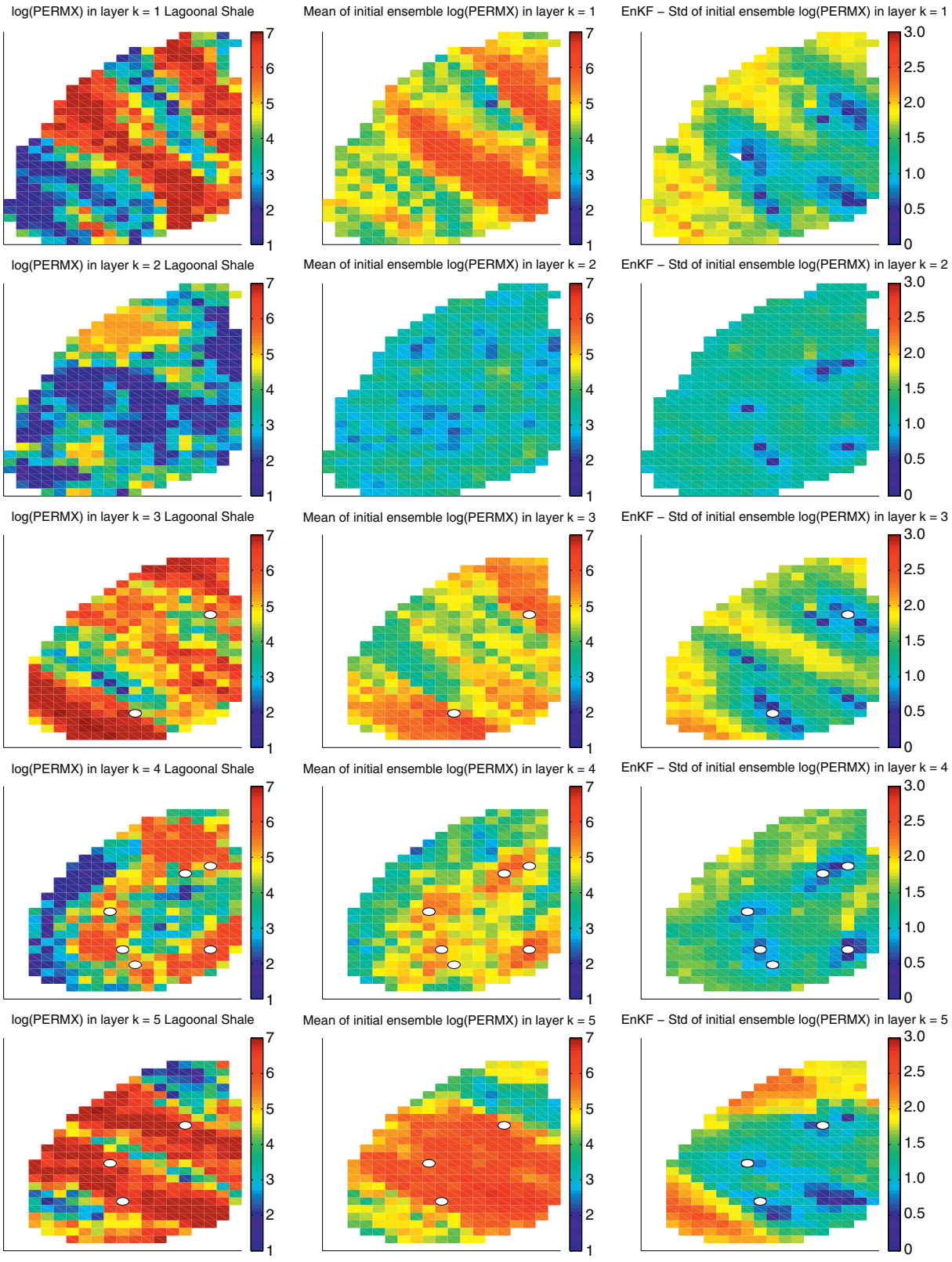

Figure 1

The horizontal log permeability. Rows 1 to 5 correspond to layers 1 to 5. The left column shows the true field and the middle and the right columns show the mean of the initial ensemble and its standard deviation, respectively.

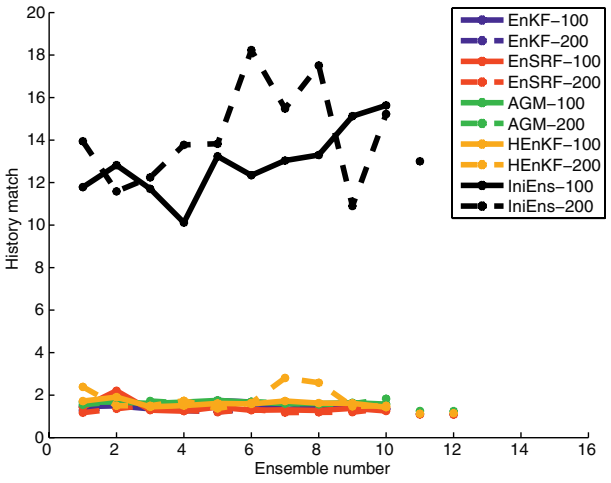

Figure 2

Objective function values (*Eq. 31, 32*) obtained for the 22 ensembles.

TABLE 2

Mean and standard deviation of the objective function values in Figure 2

Method	*J*	2σ
IniEns-100	13	3
IniEns-200	14	5
IniEns-1 000	12.999	-
IniEns-2 000	12.999	-
EnKF-100	1.5	0.3
EnKF-200	1.3	0.2
EnKF-1 000	1.1038	-
EnKF-2 000	1.1007	-
EnSRF-100	1.4	0.6
EnSRF-200	1.3	0.2
EnSRF-1 000	1.0924	-
EnSRF-2 000	1.0877	-
HEnKF-100	1.6	0.3
HEnKF-200	1.9	1
HEnKF-1 000	1.1261	-
HEnKF-2 000	1.1491	-
AGM-100	1.6	0.1
AGM-200	1.7	0.2
AGM-1 000	1.2514	-
AGM-2 000	1.2471	-

Figure 3 shows the RMSE between the analyzed ensemble and the true state (*Eq. 33*), as a function of time, for the horizontal permeability. Subfigure a) shows the results using the ensembles with 100 members, b) shows the results using the ensembles with 200 members, c) shows the mean of the results with 100 and 200 members and d) shows the result with 1 000 and 2 000 ensemble members. Considering the RMSE values in Figure 3, all methods provide very good results for all ensemble sizes and all methods improve with an increasing number of ensemble members. Some differences are seen though; especially, we see that the AGM and the HEnKF provide better results than the two other methods; the RMSE values decrease as a function of time and the variance is lower for the AGM and HEnKF. We also notice that the EnKF and the EnSRF need 2 000 ensemble members to provide comparable results to the AGM and the HEnKF. The same conclusions are drawn looking at the corresponding plots for vertical permeability and porosity (not shown). In the following, two paragraphs when discussing ensemble spread, distance to the true and ensemble shift, we will limit the discussion to the horizontal permeability, as the results for vertical permeability and porosity are similar.

In Figure 4, the dashed lines show the ensemble spread (*Eq. 35*) and the solid lines show the distance between the mean of the ensemble and the truth (*Eq. 34*). In the figure, a) shows the results for the ensembles with 100 members, b) shows the results for the ensembles with 200 members, c) shows the mean of the ones with 100 members, d) shows the mean of the ones with 200 members, e) shows the result of the ensemble with 1 000 members and f) shows the results from the ensemble with 2 000 members. As discussed above, we would like to maintain the ensemble spread and at the same time approach the true field. We see that the results improve with ensemble size for all the methods (comparing subfigures a) and b)); the ensemble spread increases (dashed lines) and the distance to the true field is reduced (solid lines). The AGM provides the highest ensemble spread of all the methods. The EnKF does the worst job with regards to maintaining the spread. Let us now consider the solid lines: we would like the distance to the truth to be as low as possible. From Figure 4, it is clear that the AGM and HEnKF outperform the EnSRF and EnKF.

Figure 5 shows how far the analyzed ensemble moves away from the initial ensemble as a function of time (*Eq. 36*). As the initial ensemble is a sample from the prior distribution, it would be preferable to obtain low values for this measure, provided that the history match is satisfying. From the figure, we see that the AGM is closest to the initial ensemble, then comes the HEnKF, then the EnSRF and furthest away from the initial ensemble is the EnKF. The increasing ensemble size has a positive and comparable-sized effect on all filters.

As an example of how the estimated fields look, we consider the horizontal log permeability for layer 5 for one of the ensembles with 100 members. Figure 6 shows the mean of the estimated ensemble at the final time step (left) and its standard deviation (right). Rows 1 to 4 correspond to the results achieved by the EnKF, EnSRF, HEnKF and AGM, respectively. The corresponding true field, mean and standard deviation of the initial ensemble are shown

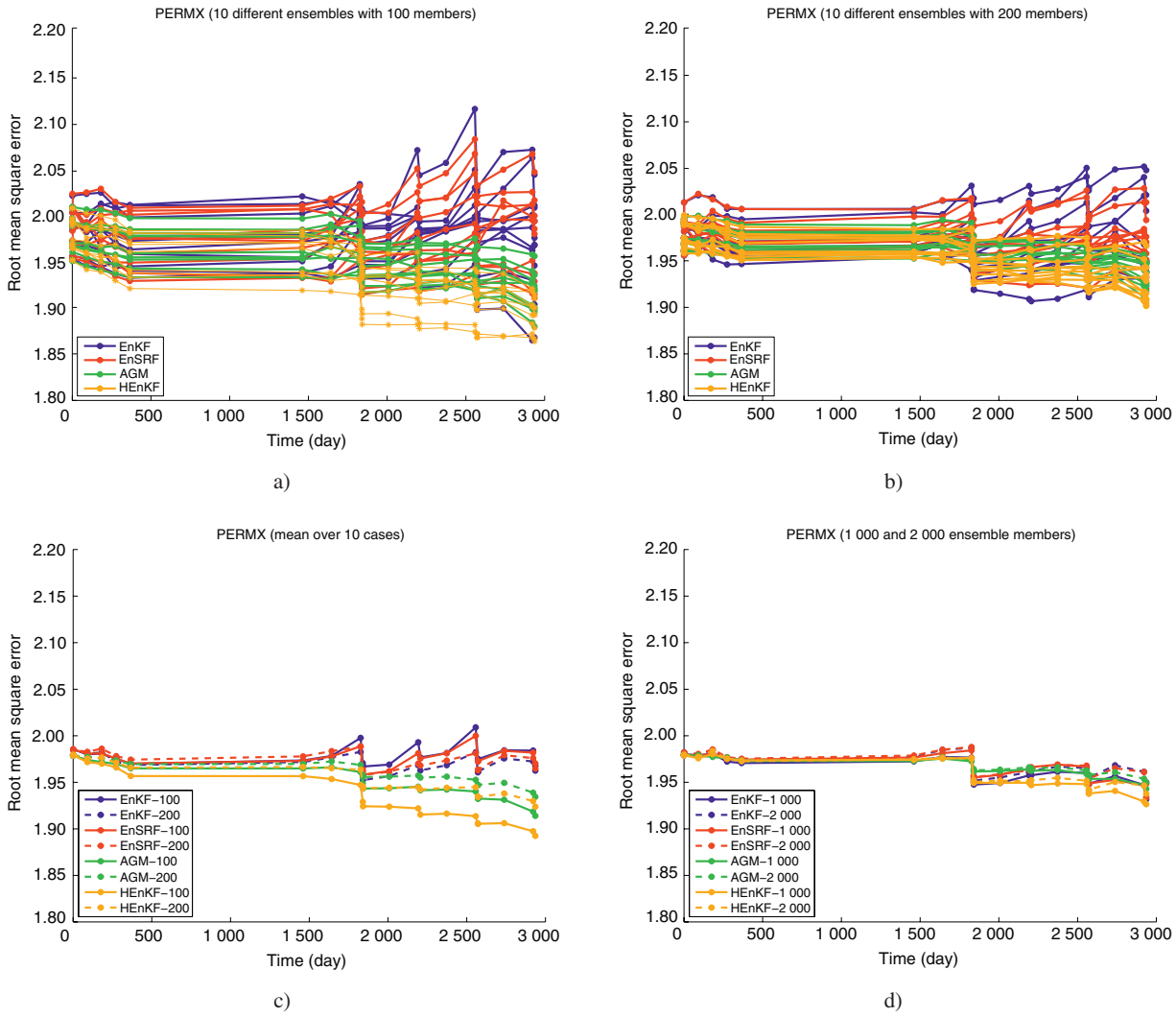

Figure 3

RMSE between the estimated and the true horizontal permeability (*Eq. 33*).

in Figure 1, bottom row. The estimated fields and the standard deviations obtained by the different methods are quite similar, which is expected for PUNQ-S3 due to the good initial ensemble. Comparing with the true field and the mean of the initial ensemble in Figure 1, bottom row, we see, however, that the EnKF has moved furthest away from the initial mean and especially at the top right of the reservoir, we see some high updates. The HEnKF and the AGM prevent the very high updates close to the boundary of the reservoir. We also see that the EnKF estimate has the lowest standard deviation of all the methods close to the boundary of the reservoir. Comparing the standard deviation of the initial ensemble (*Fig. 1*, bottom row, right figure) with the standard deviation of the estimated fields, we see that the standard deviation close to the wells is reduced by all the methods. This is expected as the assimilation of production data provides information for the flooded area.

We now turn to the second period of the PUNQ-S3 exercise. For all the 22 ensembles used for all the 4 filters, the estimated static variables at the end of the first period (8.5 years) are used as input in the simulator together with the initial equilibrium for the dynamic states and the simulator is run from 0 to 16.5 years. The Total Cumulative Oil Production (OPT) at 16.5 years is compared in Figures 7 and 8 by plotting the empirical Cumulative Distribution Function (cdf), of it. The true value is represented by the black vertical line. In Figure 7, we see the result for the EnKF in a), EnSRF in b), AGM in c) and HEnKF in

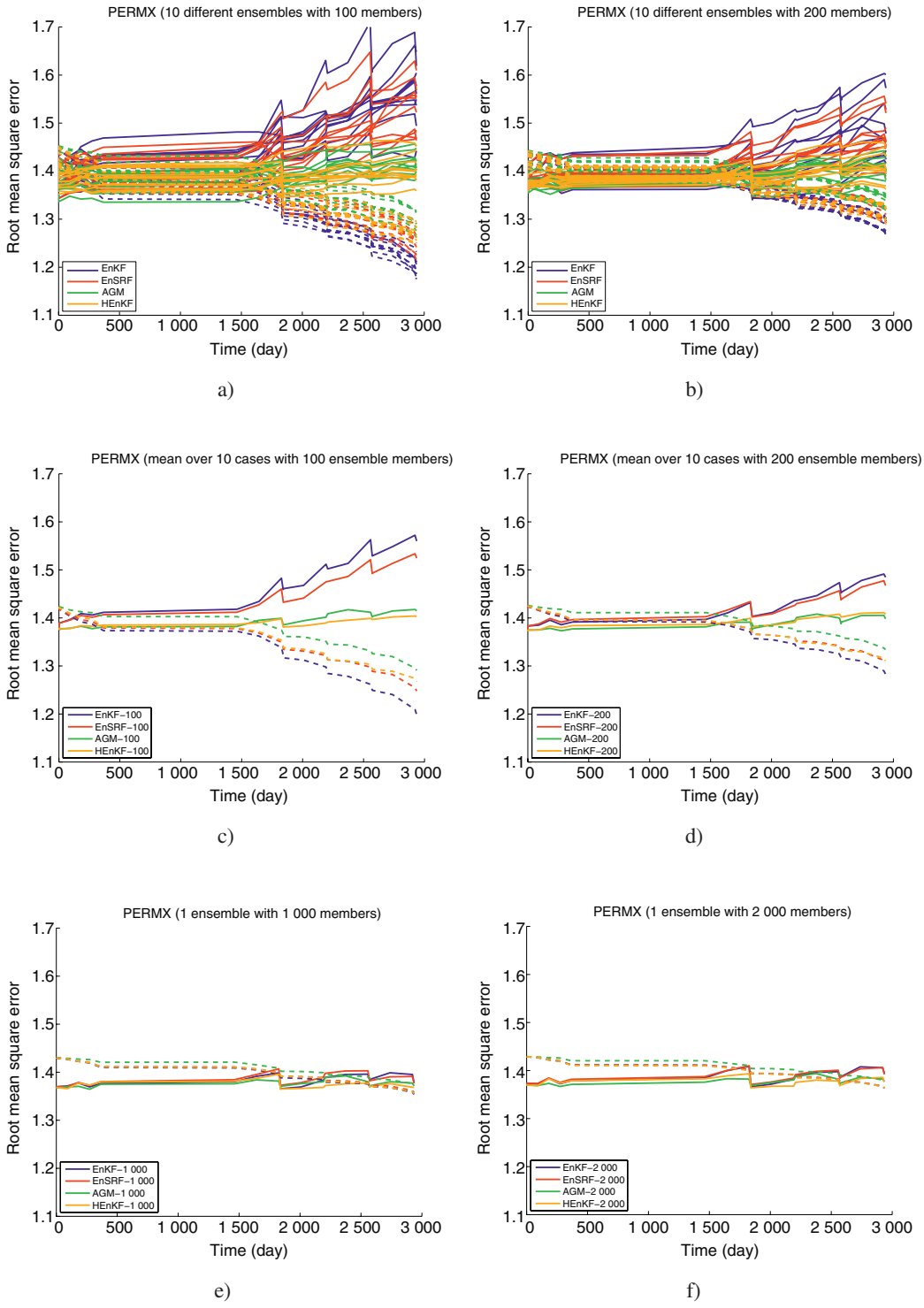

Figure 4

Dashed lines: RMSE between the mean of the ensemble and the ensemble (ensemble spread, *Eq. 35*). Solid lines: RMSE between the mean of the estimated ensemble and the true (distance from the true, *Eq. 34*). Results for estimated horizontal permeability.

d), and the results from the ensembles with 100 members are plotted in color while the results from the ensembles with 200 members are plotted by black dashed lines. For all the filters and for all the ensembles, the cdfs are closely distributed around the true value. Also, for all the filters, increasing the ensemble size seems to have a positive effect.

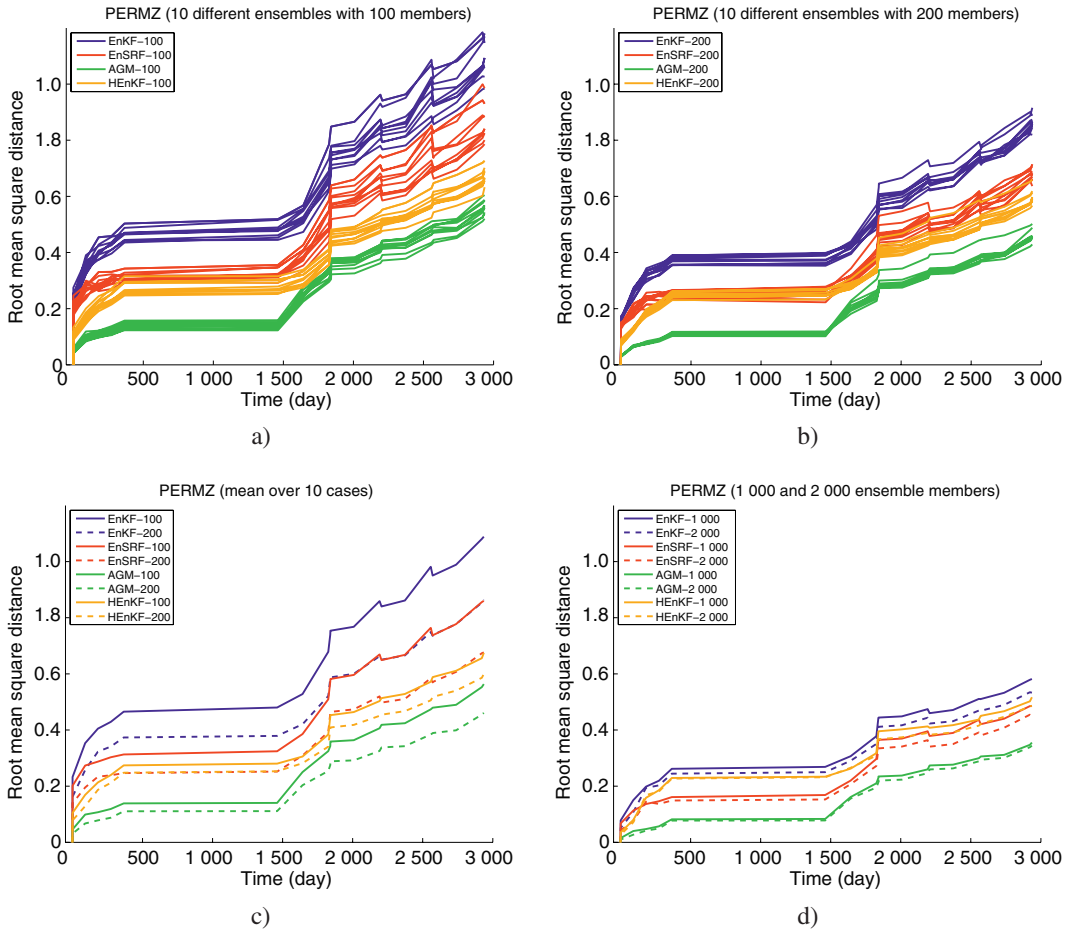

Figure 5

RMSE between the initial ensemble and the ensemble members for the horizontal permeability (*Eq. 36*).

We also see that the AGM c) and the HEnKF d) produce cdfs that are more internally consistent than the cdfs provided by the EnKF a) and the EnSRF b); this inconsistency of the forecasted cdfs provided by EnKF was also noted in Lorentzen *et al.* [25]. In Figure 8, we compare the mean cdfs with the cdfs provided with 1 000 and 2 000 ensemble members. We see that all the filters provide good results; still, the AGM is the most consistent, while the EnKF is the least consistent.

CONCLUSION

In this paper, we have compared the EnKF with the performance of the ensemble square root filter (EnSRF), the EnKF with localization (HEnKF) and the newly proposed adaptive Gaussian mixture filter (AGM) on a 3D nonlinear reservoir model. This is the first time the EnKF and the EnSRF have been compared on a high-dimensional nonlinear field case.

To perform statistical analysis of the performance of the different filters, each method was tested on several different initial ensembles. The results are evaluated by statistical measures considering the history match, the estimated ensemble and the predictability when forecasting. We see that the history match of the data provided by a rerun of the estimated ensemble is quite comparable for all the filters. The differences among the filters are, however, clearly seen when considering the quality of the ensemble and the predictability when forecasting.

Overall, we see that the AGM and HEnKF work better than the EnSRF and EnKF. The EnSRF seems to have a slightly better performance than the EnKF. However, the introduction of a localization procedure (as in the HEnKF) seems to be much more influential than replacing the EnKF with the EnSRF. Also, the potential of the AGM is illustrated by the results obtained here, even without having too much knowledge about how to select the parameter h. It should also be noted that the AGM could be extended to include localization.

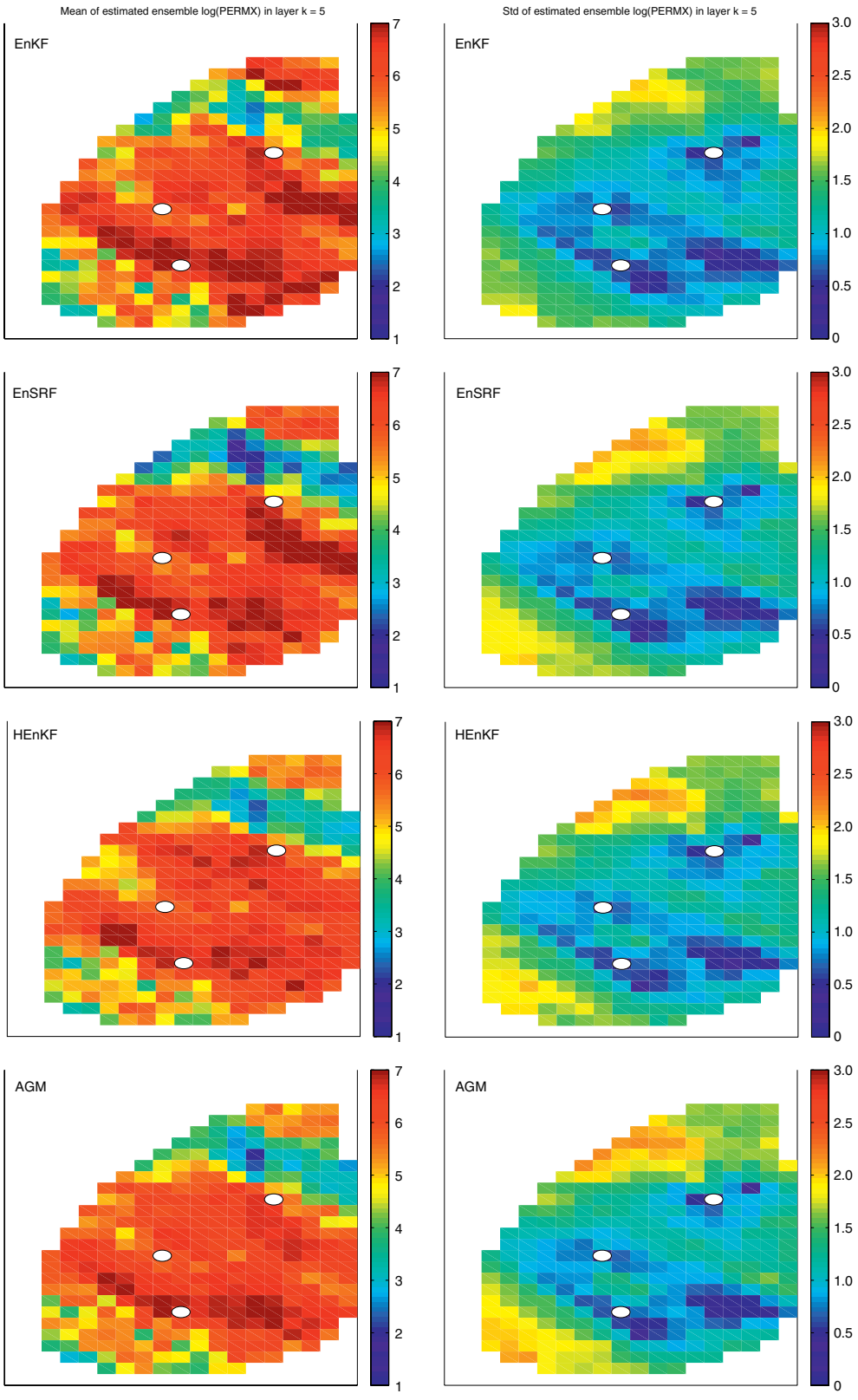

Figure 6

The horizontal log permeability for layer 5. Mean of estimated ensemble (right) and its standard deviation (left). Rows 1 to 4 show the EnKF, EnSRF, HEnKF and AGM, respectively.

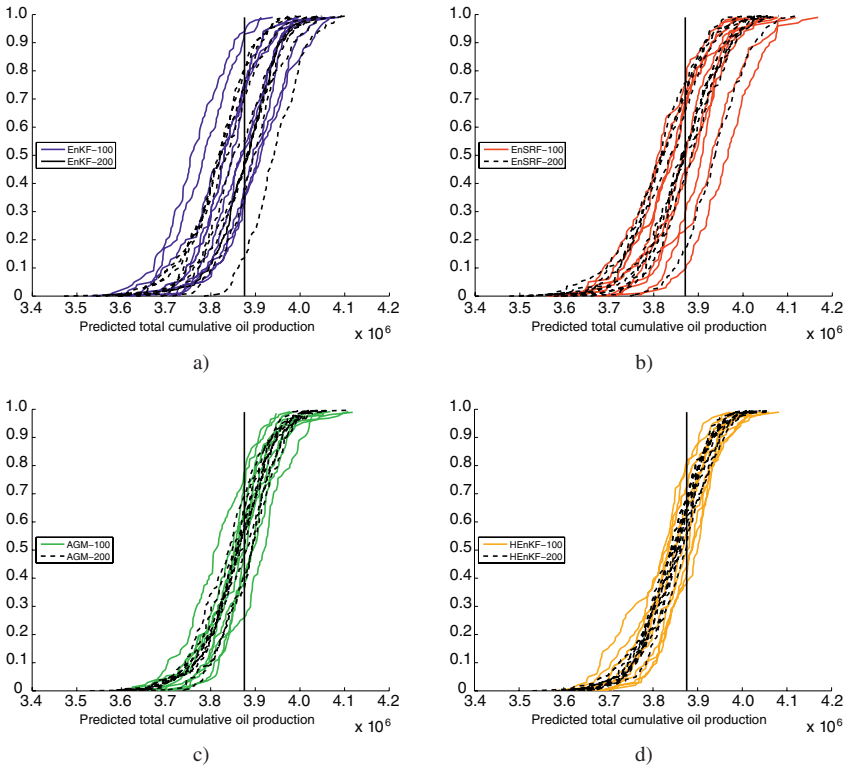

Figure 7

Predicted total cumulative oil production after forecast in Period 2; results for all ensembles with 100 and 200 members.

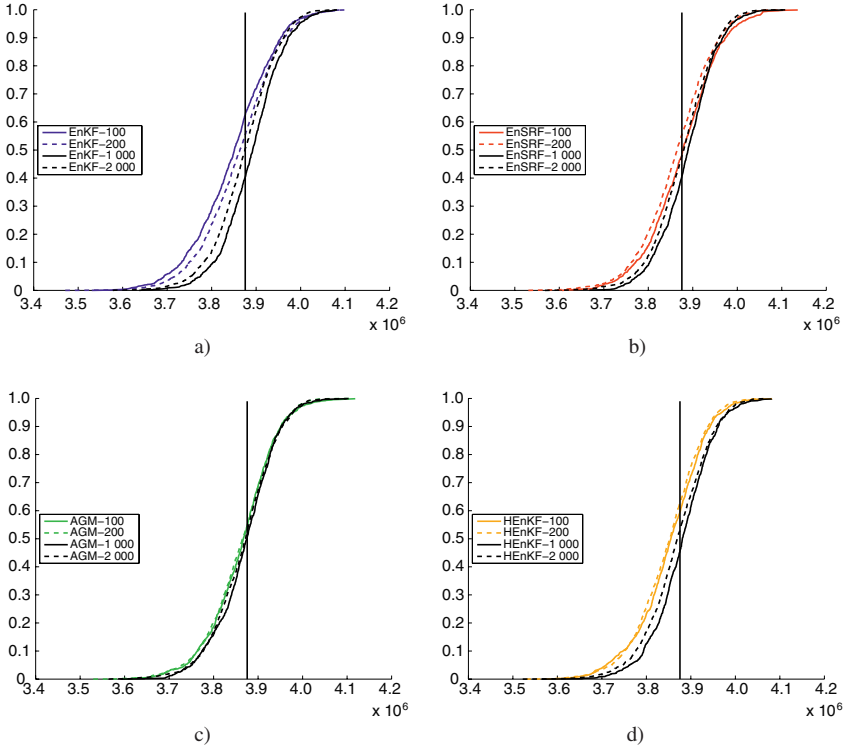

Figure 8

Predicted total cumulative oil production after forecast in Period 2. Mean of the ten ensembles with 100 and 200 members (color) compared with the ones with 1 000 and 2 000 members.

ACKNOWLEDGEMENTS

The authors would like to thank the *Research Council of Norway* (PETROMAX) and industrial participants of the project "Reservoir characterization using Ensemble Kalman filter", *Conoco Phillips*, *ENI*, *GDF SUEZ* and *Total* for providing financial support. We would also like to thank *Schlumberger* for providing us with academic software licenses for Eclipse.

REFERENCES

1 Evensen G. (1994) Sequential data assimilation with a nonlinear quasi-geostrophic model using Monte Carlo methods to forecast error statistics, *J. Geophys. Res.* **99**, C5, 10, 143, 162.

2 Lorentzen R.J., Kåre Fjelde K., Frøyen J., Lage A.C.V.M., Nævdal G., Vefring E.H. (2001) Underbalanced and low-head drilling operations: Real time interpretation of measured data and operational support, *SPE Annual Technical Conference and Exhibition*, 30 September-3 October, *SPE Paper* 71384.

3 Nævdal G., Mannseth T., Vefring E.H. (2002) Near-well reservoir monitoring through ensemble Kalman filter, *SPE/DOE Improved Oil Recovery Symposium*, Tulsa, Oklahoma, 13-17 April, *SPE Paper* 75235.

4 Haugen V., Natvik L.J., Evensen G., Berg A., Flornes K., Nævdal. G. (2006) History matching using the ensemble Kalman filter on a North Sea field case, *SPE Annual Technical Conference and Exhibition*, San Antonio, Texas, 24-27 Sept. Society of Petroleum Engineers, *SPE Paper* 102430.

5 Evensen G., Hove J., Meisingset H.C., Reiso E., Seim K.S., Espelid Ø. (2007) Using the EnKF for assisted history matching of a North Sea reservoir model, *SPE Reservoir Simulation Symposium*, Woodlands, Texas, 26-28 February, Society of Petroleum Engineers, *SPE Paper* 106184.

6 Bianco A., Cominelli A., Dovera L., Naevdal G., Vallès B. (2007) History matching and production forecast uncertainty by means of the ensemble Kalman filter: A real field application, *SPE Europec/EAGE Annual Conference and Exhibition*, London, UK, 11-14 June, Society of Petroleum Engineers, *SPE Paper* 107161.

7 Aanonsen S.I., Naevdal G., Oliver D.S., Reynolds A.C., Vallès B. (2009) The ensemble Kalman filter in reservoir engineering – a review, *SPE J.* **14**, 3, 393-412.

8 Seiler A., Aanonsen S.I., Evensen G., Rivenæs J.C. (2010) Structural surface uncertainty modeling and updating using the ensemble Kalman filter, *SPE J.* **15**, 4, 1062-1076.

9 Chen Y., Oliver D.S. (2012) Localization of ensemble-based control-setting updates for production optimization, *SPE J.* **17**, 1, 122-136.

10 Lorentzen R.J., Flornes K.M., Nævdal G. (2012) History matching channelized reservoirs using the ensemble Kalman filter, *SPE J.* **17**, 1, 137-151.

11 Verlaan M., Heemink A.W. (2001) Nonlinearity in data assimilation applications: A practical method for analysis, *Mon. Weather Rev.* **129**, 6, 1578-1589.

12 Bishop C.H., Etherton B.J., Majumdar S.J. (2001) Adaptive sampling with the ensemble transform Kalman filter. Part I: Theoretical aspects, *Mont. Weather Rev.* **129**, 420-436.

13 Tippett M.K., Anderson J.L., Bishop C.H., Hamill T.M., Whitaker J.S. (2003) Ensemble square-root filters, *Mon. Weather Rev.* **131**, 7, 1485-1490.

14 Vallès B., Nævdal G. (2009) Revisiting Brugge case study using a hierarchical ensemble Kalman filter, *International Petroleum Technology Conference*, Doha, Qatar, 7-9 Dec., IPTC-14074.

15 Anderson. J.L. (2007) Exploring the need for localization in ensemble data assimilation using a hierarchical ensemble filter, *Physica D* **230**, 99-111.

16 Stordal A.S., Karlsen H.A., Nævdal G., Skaug H.J., Vallès B. (2011) Bridging the ensemble Kalman filter and particle filters: the adaptive Gaussian mixture filter, *Comput. Geosci.* **15**, 2, 293-305.

17 Burgers G., van Leeuwen P.J., Evensen G. (1998) On the analysis scheme in the ensemble Kalman filter, *Mon. Weather Rev.* **126**, 1719-1724.

18 Houtekamer P.L., L.H. Mitchell (1998) Data assimilation using an ensemble Kalman filter technique, *Mon. Weather Rev.* **126**, 796-811.

19 Whitaker J.S., Hamil T.M. (2002) Ensemble data assimilation without perturbed observations, *Mon. Weather Rev.* **130**, 1913-1924.

20 Sakov P., Oke. P.R. (2008) Implications of the form of the ensemble transformation in the ensemble square root filters, *Mon. Weather. Rev.* **136**, 1042-1053.

21 Julier S.J., Uhlmann J.K. (1997) A new extension to the Kalman filter to nonlinear systems, *Proceedings of AeroSens: The 11th International Symposium on Aerospace/Defense Sensing, Simulation and Controls*, Orlando, Florida, 20-25 Avril.

22 Floris F.J.T., Bush M.D., Cuypers M., Roggero F., Syversveen A.R. (2001) Methods for quantifying the uncertainty of production forecasts: a comparative study, *Petrol. Geosci.* **7**, 87-96.

23 PUNQ-S3 (2012) website: http://www3.imperial.ac.uk/earthscienceandengineering/research/perm/punq-s3model.

24 Deutsch C.V., Journel A.G. (1998) *GSLIB Geostatistical Software Library and User's Guide*, Applied Geostatistics Series, Oxford University Press, second edition.

25 Lorentzen R.J., Nævdal G., Vallès B., Berg A.M., Grimstad A.-A. (2005) Analysis of the ensemble Kalman filter for estimation of permeability and porosity in reservoir models, *SPE Annual Technical Conference and Exhibition*, Dallas, Texas, 9-12 October, *SPE Paper* 96375.

Final manuscript received in June 2012
Published online in November 2012